A minimisation approach for computing the ground state of Gross–Pitaevskii systems

Marco Caliari [a,*], Alexander Ostermann [b], Stefan Rainer [b], Mechthild Thalhammer [b]

[a] *Dipartimento di Informatica, Università degli Studi di Verona, Ca' Vignal 2, Strada Le Grazie 15, I–37134 Verona, Italy.*

[b] *Institut für Mathematik, Leopold–Franzens Universität Innsbruck, Technikerstraße 13/7, A–6020 Innsbruck, Austria.*

Abstract

In this paper, we present a minimisation method for computing the ground state of systems of coupled Gross–Pitaevskii equations. Our approach relies on a spectral decomposition of the solution into Hermite basis functions. Inserting the spectral representation into the energy functional yields a constrained nonlinear minimisation problem for the coefficients. For its numerical solution, we employ a Newton-like method with an approximate line-search strategy. We analyse this method and prove global convergence. Appropriate starting values for the minimisation process are determined by a standard continuation strategy. Numerical examples with two- and three-component two-dimensional condensates are included. These experiments demonstrate the reliability of our method and nicely illustrate the effect of phase segregation.

Key words: Nonlinear Schrödinger equations, Ground state, Spectral methods, Minimisation

1 Introduction

The field of low-temperature physics has been fascinating and inspiring many scientists, in particular in the last decade, see [16] and references given therein. Memorable achievements were the first experimental realisations [1,19,22] of a single Bose–Einstein Condensate (BEC) in 1995, and of BECs for a mixture

* Corresponding author.
Email address: marco.caliari@univr.it (Marco Caliari).

of two and three different interacting atomic species, respectively. Mathematically, BECs are modelled by nonlinear time-dependent Schrödinger equations; more precisely, the order parameters of the condensates are solutions of a system of coupled Gross–Pitaevskii Equations (GPEs, [17,20]).

In the present paper, we are concerned with computing the *ground state* of a system of GPEs, a special solution of minimal energy. To this purpose, as suggested in [5], we directly minimise the energy functional. We mention that an alternative approach for the ground state computation is provided by the imaginary time method which can also be considered as a steepest descent method, see [2,3,25] e.g., resulting in a parabolic evolution equation. Besides, an optimal damping algorithm based on the inverse power method is used in [11]; then, the conjugate gradient method is applied for the solution of the arising linear systems. We do not exploit these and other ([12,23]) approaches here. Our objectives are twofold. In a general context, we present a Newton-like method for the numerical solution of a constrained minimisation problem and study its convergence. Moreover, we apply the minimisation approach specifically to a system of GPEs to simulate the ground state solution. Numerical results for two- and three-component two-dimensional condensate illustrating the effect of phase segregation [6,7,24] are provided.

The structure of the paper is as follows. In Section 2, we first introduce the system of GPEs in a normalised form and then state the minimisation problem. To avoid technicalities, we give a detailed description for the case of a single equation and then sketch the extension to systems. Our approach relies on a spectral decomposition of the ground state solution into Hermite basis functions (see also [4,10]); we point out that similar ideas could be used in combination with Fourier techniques or other spectral methods. Inserting the resulting representation into the energy functional leads to a constrained nonlinear minimisation problem for the spectral coefficients. Section 3 is devoted to the description and analysis of a numerical method for the minimisation problem. We use a Newton-like method involving an approximate line-search strategy and continuation techniques. Finally, in Section 4, we illustrate the capability of our method by three numerical examples for systems of two or three coupled Gross–Pitaevskii equations in two space dimensions.

2 Ground state of Gross–Pitaevskii systems

In this section, we present a constrained minimisation approach for computing the ground state of systems of coupled Gross–Pitaevskii equations. For our purposes, it is useful to employ a normalised form of the problem which we introduce in Section 2.1. As the discussion of the general case would involve additional technicalities, we first restrict ourselves to the case of a sin-

gle Gross–Pitaevskii equation; the extension to systems of coupled Gross–Pitaevskii equations is then sketched in Section 2.4. For the convenience of the reader, we further recall basic results on Hermite functions in Section 2.2.

We henceforth employ the vector notation $x = (x_1, \dots, x_d) \in \mathbb{R}^d$ and denote by Δ the d-dimensional Laplacian with respect to x. The Lebesgue space $L^2 = L^2(\mathbb{R}^d, \mathbb{C})$ of square integrable complex-valued functions is endowed as usual with the scalar product $(\cdot \,|\, \cdot)_{L^2}$ and the associated norm $\|\cdot\|_{L^2}$ given by

$$(f \,|\, g)_{L^2} = \int_{\mathbb{R}^d} f(x)\overline{g(x)}\, \mathrm{d}x, \quad \|f\|_{L^2} = \sqrt{(f \,|\, f)_{L^2}}, \quad f, g \in L^2.$$

2.1 Gross–Pitaevskii equation

We consider the d-dimensional nonlinear Schrödinger equation

$$\begin{cases} \mathrm{i}\hbar\partial_t \Psi(x,t) = \left(-\dfrac{\hbar^2}{2m}\Delta + V(x) + \hbar^2 g\,|\Psi(x,t)|^2\right)\Psi(x,t), \\ \|\Psi(\cdot,0)\|_{L^2}^2 = N \end{cases} \tag{1}$$

where $\Psi\colon \mathbb{R}^d \times \mathbb{R}_{\geq 0} \to \mathbb{C}$, $(x,t) \mapsto \Psi(x,t)$, $V\colon \mathbb{R}^d \to \mathbb{R}$, and $\hbar$ denotes the reduced Planck's constant. In three space dimensions this equation is called Gross–Pitaevskii equation (see [17,20]) and describes the order parameter Ψ of a Bose–Einstein condensate of an atomic species of mass m and total number of particles N, trapped in an external potential V; moreover, the *coupling constant* g equals $\frac{4\pi\sigma}{m}$, with σ being the scattering length of the species. We restrict ourselves to the defocusing case, that is $\sigma \geq 0$. Since, under certain assumptions on the potential V, the equation can be reduced to lower dimension [5], we will use the same terminology and the name GPE also for the general d-dimensional case.

In the following, we employ a normalisation of (1)

$$\begin{cases} \mathrm{i}\partial_t \psi(\xi,t) = \left(-\dfrac{1}{2}\Delta + U(\xi) + \vartheta\,|\psi(\xi,t)|^2\right)\psi(\xi,t), \\ \|\psi(\cdot,0)\|_{L^2}^2 = N \end{cases} \tag{2}$$

that is obtained by the linear transformation $\xi = \sqrt{c}x$ with $\hbar c = m$. Then, setting $C\psi(\xi,t) = \Psi(x,t)$, where $C = \sqrt[4]{c^d}$, we get the GPE (2), with real potential $\hbar U(\xi) = V(x)$ and parameter $\vartheta = \hbar g C^2 \geq 0$; in (2), Δ denotes the d-dimensional Laplacian with respect to ξ. It is easy to see that the particle number N and the energy which, for the normalised GPE (2), is given by

$$E\big(\psi(\cdot,t)\big) = \left(\left(-\frac{1}{2}\Delta + U + \frac{1}{2}\vartheta\,|\psi(\cdot,t)|^2\right)\psi(\cdot,t) \,\middle|\, \psi(\cdot,t)\right)_{L^2} \tag{3}$$

are preserved quantities in time. We further assume that the energy is positive and finite.

2.2 Hermite spectral decomposition

For any integer $j \geq 0$ and real number $\gamma > 0$, we denote by $H_j^\gamma(\xi)$ the univariate Hermite polynomial of degree j, normalised with respect to the weight function $w(\xi) = \mathrm{e}^{-\gamma^2\xi^2}$. Hermite polynomials satisfy the recurrence relation

$$\begin{aligned} H_0^\gamma(\xi) = \sqrt[4]{\frac{\gamma^2}{\pi}}, \quad H_1^\gamma(\xi) = \sqrt[4]{\frac{4\gamma^6}{\pi}}\xi, \\ \sqrt{j}H_j^\gamma(\xi) = \sqrt{2}\gamma\xi H_{j-1}^\gamma(\xi) - \sqrt{j-1}H_{j-2}^\gamma(\xi), \quad j \geq 2\,. \end{aligned} \tag{4}$$

We further recall that the derivative satisfies

$$\partial_\xi H_j^\gamma(\xi) = \gamma\sqrt{2j}H_{j-1}^\gamma(\xi)\,. \tag{5}$$

The corresponding Hermite function $\mathscr{H}_j^\gamma(\xi)$ is defined through

$$\mathscr{H}_j^\gamma(\xi) = H_j^\gamma(\xi)\,\mathrm{e}^{-\frac{1}{2}\gamma^2\xi^2}\,. \tag{6}$$

Hence, the Hermite functions $(\mathscr{H}_j^\gamma)$ form an orthonormal basis of the function space $L^2(\mathbb{R})$, i.e. it holds

$$\left(\mathscr{H}_j^\gamma \,|\, \mathscr{H}_k^\gamma\right)_{L^2(\mathbb{R})} = \delta_{jk} \tag{7a}$$

with Kronecker δ_{jk}. As a consequence, for every function $\varphi \in L^2(\mathbb{R})$, the representation

$$\varphi = \sum_j \varphi_j \mathscr{H}_j^\gamma, \quad \varphi_j = \left(\varphi \,|\, \mathscr{H}_j^\gamma\right)_{L^2(\mathbb{R})} \tag{7b}$$

is valid; moreover, Parseval's equality follows

$$\|\varphi\|_{L^2(\mathbb{R})}^2 = \sum_j |\varphi_j|^2\,. \tag{7c}$$

The above relations (5) and (6) imply

$$\left(-\partial_\xi^2 + \gamma^4\xi^2\right)\mathscr{H}_j^\gamma(\xi) = 2\lambda_j\mathscr{H}_j^\gamma(\xi), \quad 2\lambda_j = \gamma^2(1+2j)\,; \tag{8}$$

that is, the Hermite functions $(\mathscr{H}_j^\gamma)$ are eigenfunctions of the differential operator $-\partial_\xi^2 + \gamma^4\xi^2$, with corresponding eigenvalues $2\lambda_j$.

Using the tensor basis of the Hermite functions

$$\mathscr{H}_j^\gamma(\xi) = H_{j_1}^{\gamma_1}(\xi_1)\cdot\ldots\cdot H_{j_d}^{\gamma_d}(\xi_d)\,\mathrm{e}^{-\frac{1}{2}(\gamma_1^2\xi_1^2+\ldots+\gamma_d^2\xi_d^2)}$$

where, with abuse of notation, now we assume $\xi = (\xi_1, \ldots, \xi_d)$ and $j = (j_1, \ldots, j_d)$, the extension to the d-variate case is straightforward. We only notice that (8) rewrites

$$(-\Delta + U^\gamma(\xi))\, \mathscr{H}_j^\gamma(\xi) = 2\lambda_j \mathscr{H}_j^\gamma(\xi), \quad 2\lambda_j = \sum_{k=1}^{d} \gamma_k^2 (1 + 2j_k)\,, \tag{9}$$

with the standard harmonic potential $U^\gamma(\xi) = \sum_{k=1}^d \gamma_k^4 \xi_k^2$.

2.3 Minimisation approach

The ground state of the GPE (2) is a solution of the form

$$\psi(\xi, t) = \mathrm{e}^{-\mathrm{i}\mu t}\, \varphi(\xi), \quad \mu \in \mathbb{R}, \quad \varphi \in L^2(\mathbb{R}^d, \mathbb{R}) \tag{10}$$

that minimises energy functional (3); in particular, it is required that φ fulfills the relations

$$\begin{aligned} &E(\varphi) = \left(\left(-\frac{1}{2}\Delta + U + \frac{1}{2}\vartheta\varphi^2 \right) \varphi \,\middle|\, \varphi \right)_{L^2} \to \ \min, \\ &G(\varphi) = \|\varphi\|_{L^2}^2 - N = 0. \end{aligned} \tag{11a}$$

In view of the computation of the chemical potential μ, we consider the Lagrange function $\mathscr{E}(\varphi, \eta) = E(\varphi) + \eta G(\varphi)$. Using the fact that the local minima of $\mathscr{E}$ are solutions of $\nabla \mathscr{E}(\varphi, \eta) = 0$, we obtain the nonlinear system

$$\left(-\frac{1}{2}\Delta + U + \vartheta\varphi^2 \right) \varphi = \eta\varphi, \quad \|\varphi\|_{L^2}^2 = N\ ; \tag{11b}$$

the first relation in (11b) implies $E(\varphi) + \frac{1}{2}\vartheta \,\|\varphi^2\|_{L^2}^2 = N\eta$. We note that the constrained nonlinear eigenvalue problem (11b) also follows by inserting the representation (10) into (2); we conclude

$$N\mu = N\eta = E(\varphi) + \frac{1}{2}\vartheta \left\|\varphi^2\right\|_{L^2}^2,$$

i.e., μ coincides with the Lagrange multiplier η.

For the numerical solution of (11a), we employ the spectral representation (7b)

truncated to $J-1$ and property (8) to rewrite (11a) as follows

$$\begin{aligned} E_\rho(\varphi) = \sum_{|j|=0}^{J-1} \lambda_j \varphi_j^2 + \rho \int_{\mathbb{R}^d} \Big(U(\xi) - \frac{1}{2} U^\gamma(\xi) \Big) \left(\sum_{|j|=0}^{J-1} \varphi_j \mathscr{H}_j^\gamma(\xi) \right)^2 \mathrm{d}\xi \\ + \frac{1}{2} \vartheta \int_{\mathbb{R}^d} \left(\sum_{|j|=0}^{J-1} \varphi_j \mathscr{H}_j^\gamma(\xi) \right)^4 \mathrm{d}\xi \quad \to \quad \min, \end{aligned} \tag{12a}$$

$$G(\varphi) = \sum_{|j|=0}^{J-1} \varphi_j^2 - N = 0 \,, \tag{12b}$$

where $|j| = \max\{j_1, \ldots, j_d\}$, and where ρ is an additional parameter. Its significance will become clear later in Section 3.3. Here, we only mention that the energy $E_\rho(\varphi)$ to be minimized corresponds to the choice $\rho = 1$. Moreover, we approximate the integrals by means of the Gauss–Hermite quadrature formula with $2J-1$ nodes; this allows the exact integration of the term in the second line of (12a).

The choice of γ clearly depends on the potential $U(\xi)$ and on ϑ. For example, the classical and widely used (in [5,11,25], e.g.) harmonic potential

$$V(x) = \frac{m}{2} \sum_{k=1}^{d} \omega_k^2 x_k^2$$

allows to have $U(\xi) \equiv \frac{1}{2} U^\gamma(\xi)$ with $\gamma_k^2 = \omega_k$, $k = 1, \ldots, d$. On the other hand, the larger ϑ is, the wider the region is where the particles are mainly concentrated. Thus, smaller values of γ_k would help, with a better matching of the exponential decay of the Hermite functions (6).

Henceforth, we write the minimisation problem (12) in the abstract form

$$\begin{aligned} &F(x) \;\to\; \min, \\ &G_l(x) = 0, \quad 1 \le l \le \ell. \end{aligned} \tag{13}$$

In the case of a single GPE, which we considered up to now, we have $\ell = 1$. The functions F and $G_1 = G$ replace the (approximated) energy functional E and the constraint, respectively; further, the unknown $x \in \mathbb{R}^n$ takes the role of finitely many spectral coefficients φ_j.

2.4 Extension to Gross–Pitaevskii systems

In this section, we sketch how the above minimisation approach for the ground state computation extends to multicomponent systems of GPEs. Let us con-

sider the system of ℓ GPEs

$$\begin{cases} \mathrm{i}\hbar\partial_t\Psi^{(l)} = \left(-\dfrac{\hbar^2}{2m_l}\Delta + V_l + \hbar^2 g_{ll}\left|\Psi^{(l)}\right|^2 + \hbar^2\sum\limits_{\substack{k=1\\k\neq l}}^{\ell} g_{lk}\left|\Psi^{(k)}\right|^2\right)\Psi^{(l)}, \\ \left\|\Psi^{(l)}\right\|_{L^2}^2 = N_l, \quad l = 1,\dots,\ell \end{cases} \tag{14}$$

describing the order parameters $\Psi^{(l)}\colon \mathbb{R}^d \times \mathbb{R}_{\geq 0} \to \mathbb{C}$, $(x,t) \mapsto \Psi^{(l)}(x,t)$ of atomic species with masses m_l, see [15] and also [11,26]. We call g_{ll} *intra-species* coupling constants and $g_{lk} = g_{kl}$, $l \neq k$ *inter-species* coupling constants; for $d = 3$, g_{lk} equals $2\pi\sigma_{lk}\frac{m_l+m_k}{m_l m_k}$, where σ_{lk} is the scattering length for the l-k species.

Again, we restrict ourselves to the defocusing case $\sigma_{lk} \geq 0$. By a linear transformation, analogously to before, system (14) takes the form

$$\begin{cases} \mathrm{i}\partial_t\psi^{(l)} = \left(-\dfrac{\hbar c}{2m_l}\Delta + U_l + \sum\limits_{k=1}^{\ell}\vartheta_{lk}\left|\psi^{(k)}\right|^2\right)\psi^{(l)}, \\ \left\|\psi^{(l)}\right\|_{L^2}^2 = N_l, \quad l = 1,\dots,\ell \end{cases} \tag{15}$$

with

$$\hbar c = \sqrt[\ell]{m_1\cdots m_\ell} \quad \text{and} \quad \vartheta_{lk} = \hbar g_{lk} C^2, \quad C = \sqrt[4]{c^d}\,.$$

Let

$$\psi = (\psi^{(1)},\dots,\psi^{(\ell)}), \quad \varphi = (\varphi^{(1)},\dots,\varphi^{(\ell)}).$$

The ground state ψ of the GPEs system (15) is a special solution

$$\psi^{(l)}(\xi,t) = \mathrm{e}^{-\mathrm{i}\mu_l t}\,\varphi^{(l)}(\xi), \quad l = 1,\dots,\ell$$

that minimises the energy functional

$$E(\varphi) = \sum_{l=1}^{\ell}\left(\left(-\frac{\hbar c}{2m_l}\Delta + U_l + \frac{1}{2}\sum_{k=1}^{\ell}\vartheta_{lk}\left|\varphi^{(k)}\right|^2\right)\varphi^{(l)}\,\middle|\,\varphi^{(l)}\right)_{L^2}.$$

The chemical potentials μ_l are given by

$$\mu_l N_l = \left(\left(-\frac{\hbar c}{2m_l}\Delta + U_l + \sum_{k=1}^{\ell}\vartheta_{lk}\left|\varphi^{(k)}\right|^2\right)\varphi^{(l)}\,\middle|\,\varphi^{(l)}\right)_{L^2}.$$

In order to compute the ground state of (15) we thus consider the constrained minimisation problem

$$\begin{aligned} &E(\varphi) \;\to\; \min, \\ &G_l(\varphi) = \left\|\varphi^{(l)}\right\|_{L^2}^2 - N_l = 0, \quad 1 \leq l \leq \ell\,. \end{aligned}$$

As before, we employ a spectral decomposition of $\varphi^{(l)}$ into a common basis of Hermite functions; truncating the infinite sums we finally get

$$\begin{aligned} E_\rho(\varphi) = \sum_{l=1}^{\ell} \Bigg[& \frac{\hbar c}{m_l} \sum_{|j|=0}^{J-1} \lambda_j \left(\varphi_j^{(l)}\right)^2 \\ & + \rho_l \int_{\mathbb{R}^d} \left(U_l(\xi) - \frac{\hbar c}{2m_l} U^\gamma(\xi) \right) \left(\sum_{|j|=0}^{J-1} \varphi_j^{(l)} \mathscr{H}_j^\gamma(\xi) \right)^2 \mathrm{d}\xi \\ & + \frac{1}{2} \sum_{k=1}^{\ell} \vartheta_{lk} \int_{\mathbb{R}^d} \left(\sum_{|j|=0}^{J-1} \varphi_j^{(k)} \mathscr{H}_j^\gamma(\xi) \right)^2 \left(\sum_{|j|=0}^{J-1} \varphi_j^{(l)} \mathscr{H}_j^\gamma(\xi) \right)^2 \mathrm{d}\xi \Bigg] \;\to\; \min, \end{aligned} \tag{16a}$$

$$G_l(\varphi) = \sum_{|j|=0}^{J-1} \left(\varphi_j^{(l)}\right)^2 - N_l = 0, \quad 1 \le l \le \ell\,. \tag{16b}$$

This results again in a minimisation problem of the form (13).

3 Constrained minimisation

For the numerical solution of the constrained minimisation problem (13), we apply a Newton-like method with line-search; the algorithm is described and analysed in the following sections. Note that in several space dimensions, a full Newton iteration is computationally expensive due to the large number of unknowns. Our approach is based on a simplified iteration where the costs of the solution of the arising linear system grow only linearly with the number of unknowns. It turns out that our new approach is more efficient than the standard Newton iteration even in one space dimension, if a higher spatial resolution is regarded, see Fig. 1.

3.1 A Newton-like method for minimisation

Let $F\colon \mathbb{R}^n \to \mathbb{R}$ and $G_1, \ldots, G_\ell : \mathbb{R}^n \to \mathbb{R}$ be sufficiently smooth functions. We aim at finding a (local) minimiser $x^\star$ of (13). For this purpose we take up an idea presented in Han [18] and consider the exact penalty function

$$P(x) = F(x) + r \sum_{i=1}^{\ell} |G_i(x)| \tag{17}$$

with an appropriate penalty parameter $r > 0$ to be chosen in Section 3.3. Denoting $\nabla G = [\nabla G_1, \ldots, \nabla G_\ell]$, we recall that a solution $x^\star$ of (13) satisfies

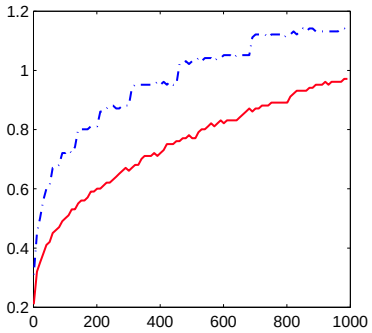

Fig. 1. CPU time in seconds necessary to compute the ground state of the one-dimensional GPE (2) with the standard harmonic potential $U(\xi) = \frac{1}{2}\xi^2$, $N = 1$, with $J = 140$ Hermite functions, as a function of ϑ. The exact Newton method (dashed line) is more expensive than our new strategy (solid line), described in Section 3.

the first order conditions

$$\nabla F(x^\star)^\mathsf{T} + y^{\star\mathsf{T}} \nabla G(x^\star)^\mathsf{T} = 0 \tag{18a}$$

$$G(x^\star) = 0 \tag{18b}$$

with a corresponding Lagrange multiplier $y^\star$. Any point $x^\star$ satisfying these first order conditions is called a *critical point* of (13).

Starting from a given approximation $x^{(k)}$ to the minimiser $x^\star$, we consider the quadratic minimisation problem $Q(x^{(k)}, H^{(k)})$

$$\nabla F(x^{(k)})^\mathsf{T} s + \frac{1}{2} s^\mathsf{T} H^{(k)} s \to \min \tag{19a}$$

subject to the linear constraints

$$G_i(x^{(k)}) + \nabla G_i(x^{(k)})^\mathsf{T} s = 0, \quad i = 1, \ldots, \ell. \tag{19b}$$

Here, $H^{(k)}$ denotes a symmetric matrix that approximates the Hessian of F. We propose to take $H^{(k)} = H(x^{(k)})$ with an appropriate function H. The precise choice of H will be discussed in Section 3.2 below. Han shows that a solution $s^{(k)}$ of (19) is a descent direction of (17), if $H^{(k)}$ is positive definite and the corresponding Lagrange multiplier is bounded by r, see [18, Thm. 3.1]. For an appropriate step length λ_k satisfying

$$P\Big(x^{(k)} + \lambda_k s^{(k)}\Big) < P\Big(x^{(k)}\Big),$$

the new approximation $x^{(k+1)}$ is defined by

$$x^{(k+1)} = x^{(k)} + \lambda_k s^{(k)}. \tag{20}$$

In order to get a globally convergent method, the step length λ_k has to satisfy additional conditions. Among the different possibilities, we consider the first

Armijo–Goldstein condition

$$P(x^{(k)} + \lambda_k s^{(k)}) \leq P(x^{(k)}) + \alpha\lambda_k \nabla P(x^{(k)})^\mathsf{T} s^{(k)} \tag{21}$$

for some fixed $0 < \alpha < 1$, independently of k. The existence of the directional derivative $\nabla P(x^{(k)})^\mathsf{T} s^{(k)}$ is verified in [18].

We employ a backtracking line-search strategy as described in [8, Sect. 6.3.2]. This turns out to be an essential feature of our method. The size of α in (21) is typically quite small. In literature, the value $\alpha = 10^{-4}$ is recommended. Starting with an initial guess $\lambda = 1$ for the step length, we reduce λ step by step by a factor $\beta \in [0.1, 0.5]$ until (21) holds. In each step of this line-search, the size of β is determined anew from a quadratic or a cubic model of the restriction of P in search direction. For details of this algorithm, see [8, Algorithm A6.3.1].

The convergence properties of our algorithm are collected in the following theorem which is obtained by a small modification of Theorem 3.2 in [18]. In contrast to [18], we use a different (non exact) line-search strategy.

Theorem 1 *Let F and $G = (G_1, \ldots, G_\ell)^\mathsf{T}$ be continuously differentiable and let the following conditions hold, where $\{x^{(k)}\}$ denotes the sequence defined in* (20)*:*

(a) The function F is bounded from below and ∇G has full rank.
(b) The matrices $H^{(k)} = H(x^{(k)})$ are positive definite, and for all critical points $x^\star$ of (13) *there exists a neighborhood where H is continuous.*
(c) The solution of each quadratic minimisation problem $Q(x^{(k)}, H^{(k)})$, given by (19)*, has a Lagrange multiplier that is bounded by r in the maximum norm.*

Then, the sequence $\{x^{(k)}\}$ converges to a critical point $x^\star$ of (13)*, or any of its accumulation points is a critical point.*

PROOF. Since F is bounded from below, the exact penalty function P has the same property. By construction, the sequence $\{P(x^{(k)})\}$ is monotonically decreasing and thus converges to $p^\star$, say. Let $x^\star$ be an accumulation point of the sequence $\{x^{(k)}\}$. Without loss of generality, we may assume that $x^{(k)}$ converges to $x^\star$. In particular, we have $\lambda_k s^{(k)} \to 0$ for $k \to \infty$.

Since F and G_i, $i = 1, \ldots, \ell$ are continuously differentiable, and $H^{(k)} = H(x^{(k)})$ with continuous H, for k sufficiently large, the corresponding solutions $s^{(k)}$ of (19) converge to $s^\star$ which solves $Q(x^\star, H(x^\star))$.

If $s^\star = 0$, then $x^\star$ obviously satisfies the first order conditions (18).

Otherwise, as $s^\star \neq 0$, we conclude from [18, Thm. 3.1] that there exists $\lambda > 0$ with $P(x^\star + \lambda s^\star) < P(x^\star)$. In accordance with our backtracking strategy, let $\lambda^\star$ be the largest $\lambda \in (0, 1]$ that satisfies the Armijo–Goldstein condition (21). Due to the continuity of the data, we have that $\lambda_k \geq \lambda^\star/2$ for k sufficiently large which contradicts $\lambda_k s^{(k)} \to 0$. $\square$

3.2 Application to the GPE

In order to apply the just described method to our constrained minimisation problem (13), we have to define the function H.

For this, we choose a singularity level $\texttt{TOL}$ and set

$$d_j(x) = \left| \frac{\partial^2 F}{\partial x_j^2} + \sum_{i=1}^{\ell} y_i \frac{\partial^2 G_i}{\partial x_j^2} \right|. \tag{22}$$

If $d_j(x) \leq \texttt{TOL}$, we modify (22) to $d_j(x) = 1$. A typical value for the singularity level is $\texttt{TOL} = 10^{-8}$. With

$$\delta(x) = \max\left(1, \texttt{TOL}\frac{\|\nabla F(x)\|_2}{\|\Delta(x)\|_2}\right), \quad \Delta(x) = \Big(d_1(x), \ldots, d_n(x)\Big)^{\mathsf{T}} \tag{23}$$

we finally define the function H as

$$H(x) = \delta(x)\mathrm{diag}\Big(d_1(x), \ldots, d_n(x)\Big). \tag{24}$$

This choice of H satisfies the conditions of Theorem 1.

In some of our examples below, the generic choice $\alpha = 10^{-4}$ in (21) required an unexpectedly high number of iterations. This happens even in the one-dimensional single-equation case for particular values of ϑ, see Fig. 2. To overcome this problem, we vary the size of α in the iteration process. After accepting a step, say step k, we update α as follows.

If $\lambda_k = 1$ and $\nabla P(x^{(k)})^{\mathsf{T}} s^{(k)} < 0$, we increase α according to

$$\alpha^{\mathrm{new}} = \min\Big(\widehat{\alpha}, 1.25\alpha, 0.99\Big), \quad \widehat{\alpha} = \frac{P(x^{(k+1)}) - P(x^{(k)})}{\nabla P(x^{(k)})^{\mathsf{T}} s^{(k)}}; \tag{25a}$$

else, if $\lambda_k < 1$, we decrease α according to

$$\alpha^{\mathrm{new}} = \max\Big(10^{-4}, \min(\lambda, 0.75\alpha)\Big). \tag{25b}$$

If α^{new} does not admit an admissible step length in step $k+1$, we put $\alpha^{\mathrm{new}} = 10^{-4}$ and restart the line-search with $\lambda = 1$.

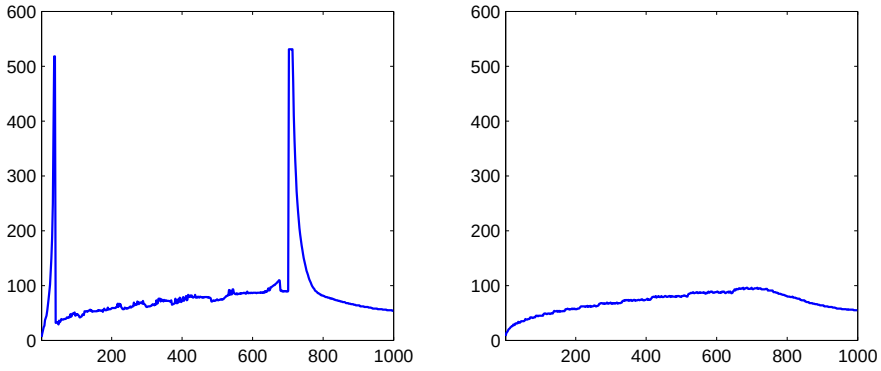

Fig. 2. Number of iterations necessary to compute the ground state of the one-dimensional GPE (2) with the standard harmonic potential $U(\xi) = \frac{1}{2}\xi^2$, $N = 1$, as a function of ϑ. The left figure displays the results obtained with the traditional choice $\alpha = 10^{-4}$, the right figure those obtained with the new strategy (25) for selecting α.

3.3 Choice of the penalty parameter and the starting values

Appropriate starting values for the local optimisation procedure are determined with the help of a continuation method. For a general overview of such methods, see [9]. In our case, we choose ϑ_{lk} and ρ_l as continuation parameters. For this purpose, we replace ϑ_{lk} by $\widehat{\vartheta}_{lk}$ in (16a) and continue, for appropriate initial values, the parameters $\widehat{\vartheta}_{lk}$ to ϑ_{lk} and ρ_l to 1. As initial values for $\widehat{\vartheta}_{lk}$, we take $\widehat{\vartheta}_{lk} = (N_l N_k)^{-1/2}$. The choice of the initial values for ρ_l is more tricky. It depends on the difference between the given and the harmonic potential. If the potentials are very close to each other, the corresponding ρ_l is chosen close to 1, with $\rho_l = 1$ for the standard harmonic potential. Otherwise, ρ_l is taken smaller.

In the first step of the continuation method, we take as starting value φ the ground state of the linear Schrödinger equation with standard harmonic potential. In the subsequent steps, we then take the solution of the previous step as starting value for φ.

For the actual values of $\widehat{\vartheta}_{lk}$ and ρ_l, we compute the ground state by using the above procedure. Thereafter, we enlarge $\widehat{\vartheta}_{lk}$ and ρ_l according to the formulas

$$\widehat{\vartheta}_{lk}^{\text{new}} = (1+\kappa)\widehat{\vartheta}_{lk}, \qquad \rho_l^{\text{new}} = (1+\kappa)\rho_l. \tag{26}$$

The size of κ in (26) has to be chosen appropriately. We take here into account the speed of convergence of the iteration. If the residual is smaller than 10^{-6} after less than three iterations, we double the value κ in the next continuation step; if the residual does not meet the condition after ten iterations, we half κ and redo the whole step; else, we keep the value of κ in the next step.

This procedure allows to determine appropriate starting values even for large values of ϑ_{lk} in a fast and reliable way.

The penalty parameter r in (17) is chosen in accordance with the size of the chemical potentials $\mu_1, \ldots, \mu_\ell$. Having computed the ground state φ of the current step, we calculate approximations to the chemical potential for $\widehat{\vartheta}_{lk}^{\text{new}}$ by using the just computed φ. The maximal value of these approximations is taken for r. This choice guarantees that r is an upper bound for the Lagrange multiplier in the step for $\widehat{\vartheta}_{lk}^{\text{new}}$.

4 Numerical implementation and illustrations

We have implemented the above algorithm in MATLAB and it can be used without any restriction also in GNU OCTAVE, version greater or equal to 3.0.0. In the present version, our code can treat coupled systems of GPEs in one or two space dimensions. Gauss–Hermite quadrature points are computed using the stable and efficient routines provided in [13,14]. Hermite functions at quadrature points are computed once and for all using the stable recurrence relation (4). The program is freely available from the authors on request.

The following examples illustrate the capability of our method. We note that the choice of the parameters is not strictly related to physical experiments. In particular, in all the numerical examples we use the same masses for all the components, but vary the scattering lengths. We emphasise however that in our implementation there is no restriction at all in using different masses. SI units are used throughout this section.

Example 1. As a first numerical example, we first consider the case of a two-component ($\ell = 2$) two-dimensional condensate, modelled by (15), each component with the same atomic species ^{87}Rb, mass $m_l = m = 1.44 \cdot 10^{-25}$, and the same number of particles $N_l = N = 10^7$. The intra-species coupling constants are $\vartheta_{11} = 1.3 \cdot 10^{-6}$ and $\vartheta_{22} = 1.3 \cdot 10^{-11}$. The potentials are scaled and off-centered harmonic potentials (see, e.g., [2]), namely

$$U_l(\xi_1, \xi_2) = \frac{1}{2}\left[(\omega_{1l}(\xi_1 - \xi_{1l}))^2 + (\omega_{2l}(\xi_2 - \xi_{2l}))^2\right]$$

with

$$\begin{aligned} &\omega_{11} = \pi, \quad \omega_{21} = \pi, \quad \xi_{11} = 0, && \xi_{21} = 0\ , \\ &\omega_{12} = 3\pi, \quad \omega_{22} = 3\pi, \quad \xi_{12} = 5 \cdot 10^{-6}, && \xi_{22} = 0\ . \end{aligned}$$

We perform four numerical experiments, with identical inter-species coupling constant ϑ_{lk}, $l \neq k$, assuming the values 0, $2.5 \cdot 10^{-7}$, $1.0 \cdot 10^{-6}$ and $2.0 \cdot 10^{-6}$, respectively. The number of Hermite functions was fixed to $J = 64$ for each direction and component, resulting in a total of $\ell J^2 = 8192$ degrees of freedom

for the spectral coefficients. The required CPU time (on a 2.2Ghz CPU) is about 2 seconds. The contour plots of the solution are given in Fig. 3.

Example 2. As a second example, we consider the case of a three-component ($\ell = 3$) two-dimensional condensate, modelled by (15), each component with the same atomic species ^{87}Rb, mass $m_l = m = 1.44 \cdot 10^{-25}$, and the same number of particles $N_l = N = 10^7$. The intra-species coupling constants are $\vartheta_{11} = \vartheta_{33} = 1.3 \cdot 10^{-5}$ and $\vartheta_{22} = 6.3 \cdot 10^{-8}$. The potentials are scaled, off-centered and rotated harmonic potentials, namely

$$U_l(\xi_1, \xi_2) = \frac{1}{2}\Big[(\omega_{1l}((\xi_1 - \xi_{1l})\cos\Omega_l + (\xi_2 - \xi_{2l})\sin\Omega_l))^2 + \\ + (\omega_{2l}((\xi_1 - \xi_{1l})\sin\Omega_l - (\xi_2 - \xi_{2l})\cos\Omega_l))^2\Big]$$

with

$$\begin{aligned}
&\omega_{11} = \frac{3}{2}\pi, \quad \omega_{21} = \pi, \quad \Omega_1 = 0, \quad \xi_{11} = 10^{-5}, \quad \xi_{21} = 0\ , \\
&\omega_{12} = \frac{3}{2}\pi, \quad \omega_{22} = \pi, \quad \Omega_2 = 0, \quad \xi_{12} = -10^{-5}, \quad \xi_{22} = 0\ , \\
&\omega_{13} = \pi, \quad \omega_{23} = 2\pi, \quad \Omega_3 = \frac{\pi}{4}, \quad \xi_{13} = 0, \quad \xi_{23} = 0\ .
\end{aligned}$$

We perform five numerical experiments, with identical inter-species coupling constant ϑ_{lk}, $l \neq k$, assuming the values 0, $1.3 \cdot 10^{-6}$, $2.5 \cdot 10^{-6}$, $5.0 \cdot 10^{-6}$ and $1.0 \cdot 10^{-5}$, respectively. The number of Hermite functions was fixed to $J = 64$ for each direction and component, resulting in a total of $\ell J^2 = 12288$ degrees of freedom for the spectral coefficients. The required CPU time is about 2 seconds. The contour plots of the solution are given in Fig. 4.

Increasing the inter-species coupling constant ϑ_{lk} clearly shows the phase segregation phenomenon (see [21,24]) already discussed and proved in [6,7] for the two-component and the three-component condensate, respectively.

Example 3. Finally, we consider again the case of a three-component two-dimensional condensate, each component with the same atomic species ^{87}Rb, mass $m_l = m = 1.44 \cdot 10^{-25}$, and the same number of particles $N_l = N = 10^7$. The intra-species coupling constants are $\vartheta_{ll} = 1.3 \cdot 10^{-5}$, $l = 1, 2, 3$ and $\vartheta_{12} = \vartheta_{21} = 0$. The potentials are scaled and strongly anisotropic harmonic potentials, namely

$$U_l(\xi_1, \xi_2) = \frac{1}{2}\Big[(\omega_{1l}\xi_1)^2 + (\omega_{2l}\xi_2)^2\Big]$$

with

$$\omega_{11} = \pi,\ \omega_{21} = 10\pi, \quad \omega_{12} = 10\pi,\ \omega_{22} = \pi, \quad \omega_{13} = \pi,\ \omega_{23} = \pi\ .$$

We perform five numerical experiments, with $\vartheta_{13} = \vartheta_{31} = \vartheta_{23} = \vartheta_{32}$ assuming the values 0, $5 \cdot 10^{-6}$, $1.3 \cdot 10^{-5}$, $2.5 \cdot 10^{-5}$ and $5 \cdot 10^{-5}$, respectively. The number of Hermite functions was fixed to $J = 70$ for each direction and

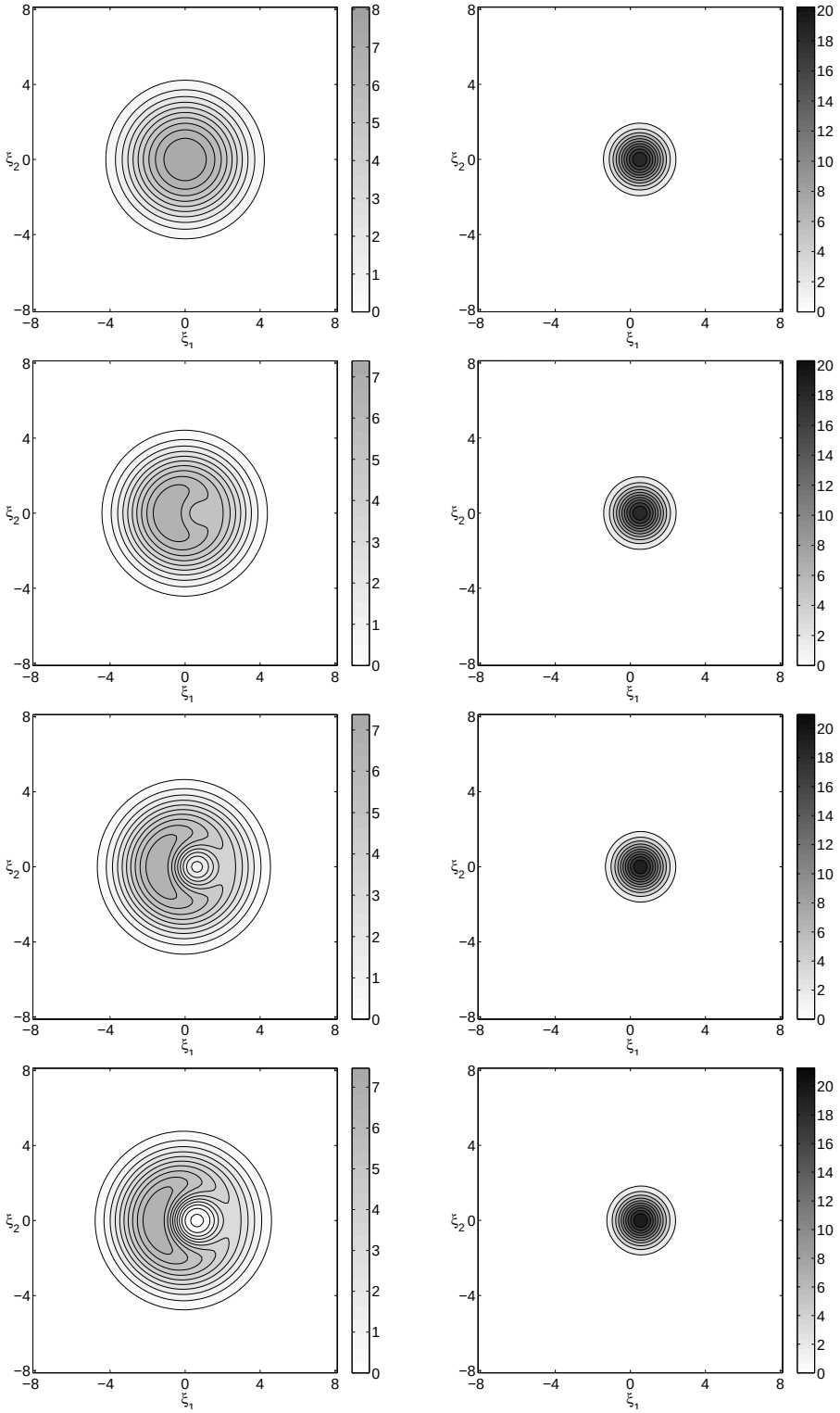

Fig. 3. Contour plots of the ground state $\left(\varphi^{(1)}(\xi), \varphi^{(2)}(\xi)\right)$ of Example 1 (left–right) for ϑ_{lk}, $l \neq k$, assuming the values 0, $2.5 \cdot 10^{-7}$, $1.0 \cdot 10^{-6}$ and $2.0 \cdot 10^{-6}$ (top–bottom). The unit length for ξ_1 and ξ_2 is 10^{-5}; the unit length for the function values is 10^7.

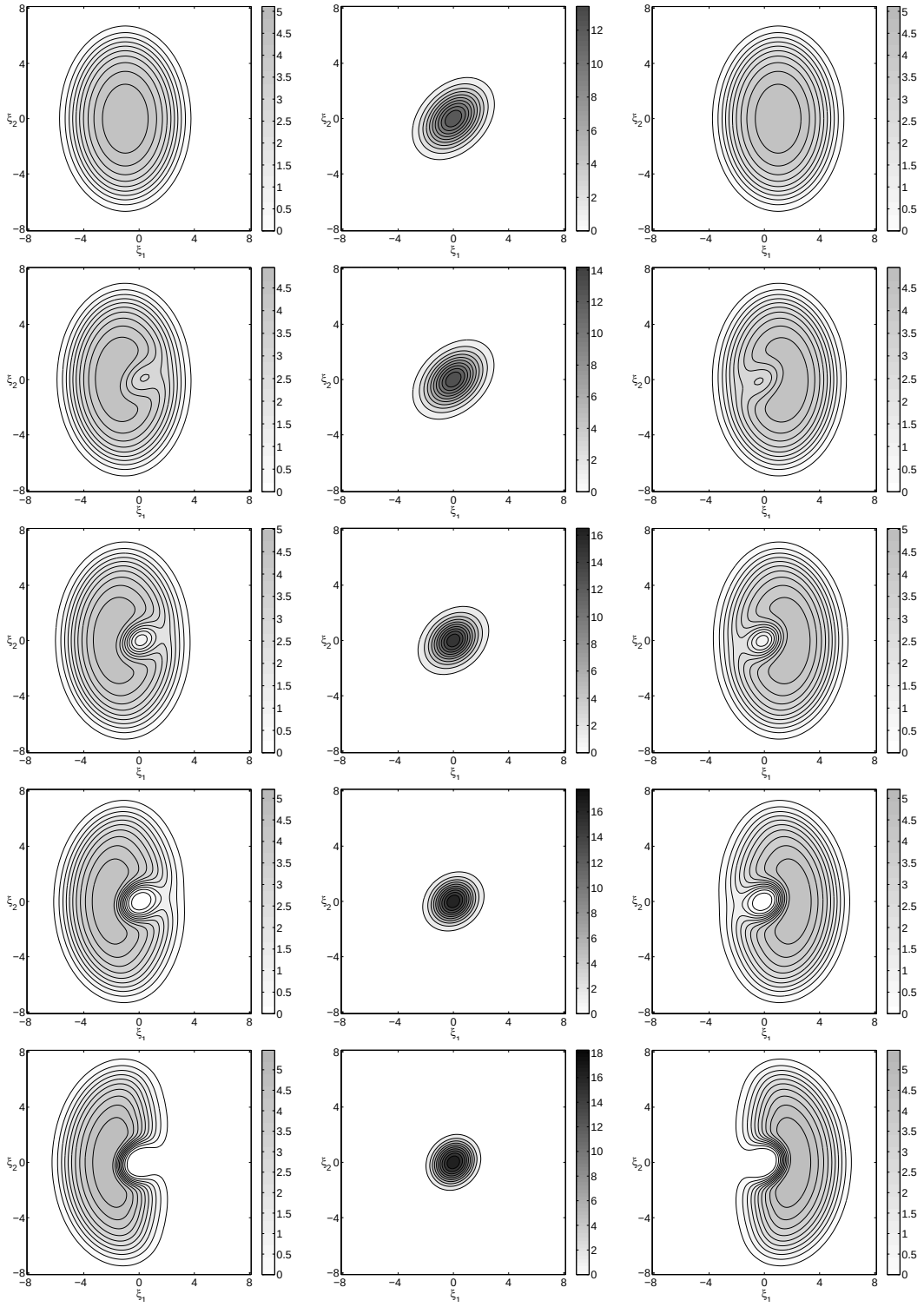

Fig. 4. Contour plots of the ground state $\left(\varphi^{(1)}(\xi), \varphi^{(2)}(\xi), \varphi^{(3)}(\xi)\right)$ of Example 2 (left–right) for ϑ_{lk}, $l \neq k$, assuming the values 0, $1.3 \cdot 10^{-6}$, $2.5 \cdot 10^{-6}$, $5.0 \cdot 10^{-6}$ and $1.0 \cdot 10^{-5}$ (top–bottom). The unit length for ξ_1 and ξ_2 is 10^{-5}; the unit length for the function values is 10^7.

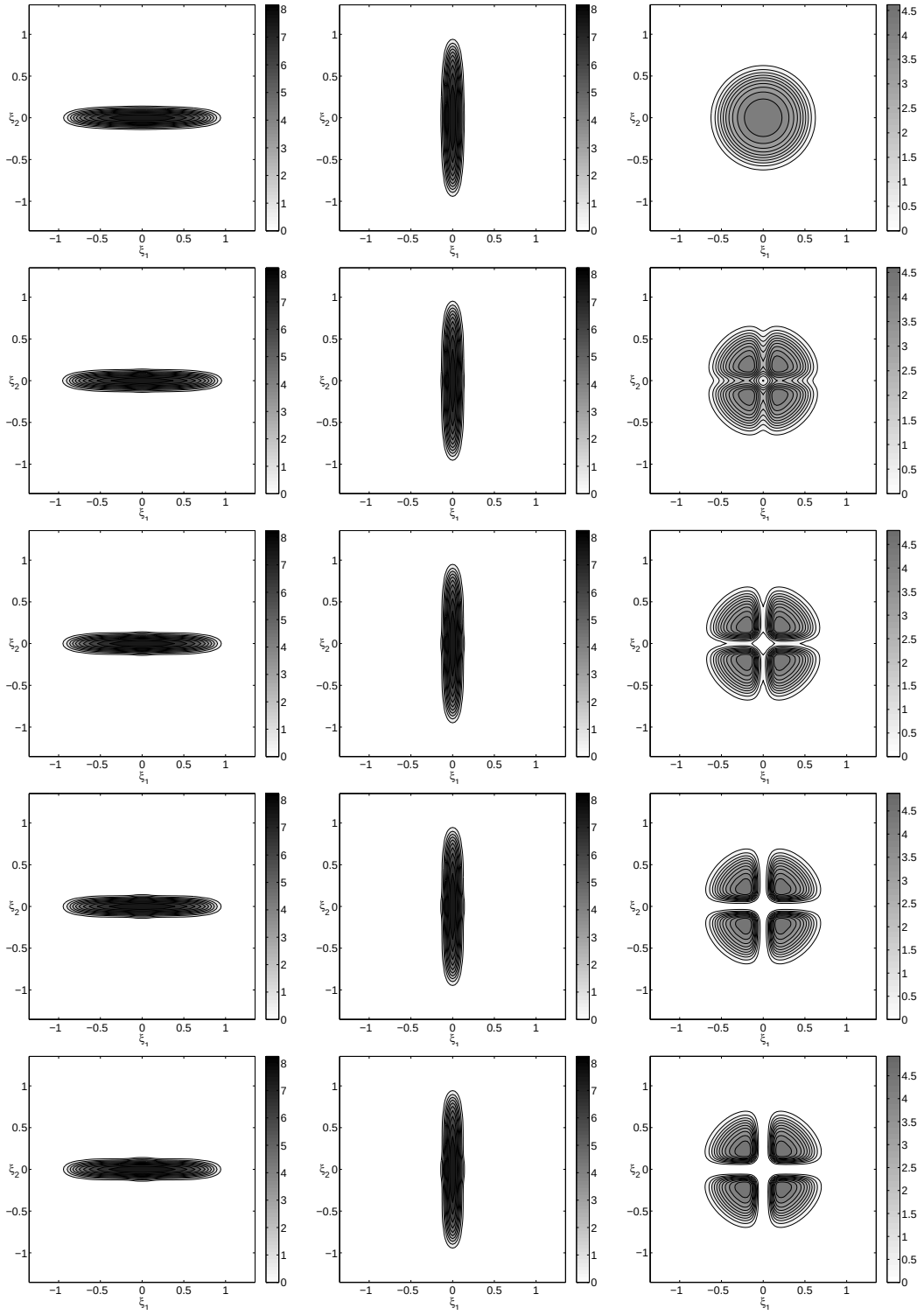

Fig. 5. Contour plots of the ground state $\left(\varphi^{(1)}(\xi), \varphi^{(2)}(\xi), \varphi^{(3)}(\xi)\right)$ of Example 3 (left–right) for $\vartheta_{13} = \vartheta_{31} = \vartheta_{23} = \vartheta_{32}$ assuming the values 0, $5 \cdot 10^{-6}$, $1.3 \cdot 10^{-5}$, $2.5 \cdot 10^{-5}$ and $5 \cdot 10^{-5}$, (top–bottom). The unit length for ξ_1 and ξ_2 is 10^{-4}; the unit length for the function values is 10^7.

component, resulting in a total of $\ell J^2 = 14700$ degrees of freedom for the spectral coefficients. The required CPU time is about 12 seconds. The contour plots of the solution are reported in Fig. 5.

5 Conclusions

In this paper, we were concerned with the numerical computation of the ground state of Gross–Pitaevskii systems. By means of a spectral discretisation, we transformed the problem into a constrained minimisation problem and employed a Newton-like method with approximate line-search for its numerical solution. The algorithm was implemented in MATLAB (and successfully tested in GNU OCTAVE); the code is available from the authors on request. The enclosed numerical examples clearly demonstrate the reliability of the new method. We point out that the presented minimisation approach is neither restricted to Gross–Pitaevskii systems nor to Hermite basis functions.

6 Acknowledgements

The authors wish to thank Marco Squassina for providing the settings used for the experiment illustrated in Fig. 5.

References

[1] M. H. Anderson, J. R. Ensher, M. R. Matthews, C. E. Wieman, E. A. Cornell, Observation of Bose–Einstein condensation in a dilute atomic vapor, Science 269 (5221) (1995) 198–201.

[2] W. Bao, Ground states and dynamics of multicomponent Bose–Einstein condensates, Multiscale Model. Simul. 2 (2) (2004) 210–236.

[3] W. Bao, Q. Du, Computing the ground state solution of Bose–Einstein condensates by a normalized gradient flow, SIAM J. Sci. Comput. 25 (5) (2004) 1674–1697.

[4] W. Bao, J. Shen, A fourth-order time-splitting Laguerre–Hermite pseudospectral method for Bose–Einstein condensates, SIAM J. Sci. Comput. 26 (6) (2005) 2010–2028.

[5] W. Bao, W. Tang, Ground-state solution of Bose–Einstein condensate by directly minimizing the energy functional, J. Comp. Phys. 187 (2003) 230–254.

[6] M. Caliari, M. Squassina, Location and phase segregation of ground and excited states for 2D Gross–Pitaevskii systems, Dyn. Partial Differ. Equ. 5 (2) (2008) 117–137.

[7] M. Caliari, M. Squassina, Spatial patterns for the three species Gross–Pitaevskii system in the plane, Electron. J. Diff. Eqns. 2008 (79) (2008) 1–15.

[8] J. E. Dennis, R. B. Schnabel, Numerical Methods for Unconstrained Optimization and Nonlinear Equations, SIAM, Philadelphia, 1998.

[9] P. Deuflhard, Newton Methods for Nonlinear Problems, Springer, Berlin, 2004.

[10] C. M. Dion, E. Cancès, Spectral method for the time-dependent Gross–Pitaevskii equation with a harmonic trap, Phys. Rev. E 67 (2003) 046706.

[11] C. M. Dion, E. Cancès, Ground state of the time-independent Gross–Pitaevskii equation, Comput. Phys. Commun. 177 (10) (2007) 787–798.

[12] M. Edwards, R. J. Dodd, C. W. Clark, P. A. Ruprecht, K. Burnett, Properties of a Bose–Eistein condensate in an anisotropic harmonic potential, Phys. Rev. A 53 (4) (1996) 1950–1953.

[13] W. Gautschi, Orthogonal Polynomials: Computation and Approximation, Clarendon Press, Oxford, 2004.

[14] W. Gautschi, Orthogonal polynomials (in Matlab), J. Comput. Appl. Math. 178 (1–2) (2005) 215–234.

[15] R. Graham, D. Walls, Collective excitations of trapped binary mixtures of Bose–Einstein condensed gases, Phys. Rev. A 57 (1) (1998) 484–487.

[16] R. Grimm, Low-temperature physics: A quantum revolution, Nature 435 (2005) 1035–1036.

[17] E. P. Gross, Structure of a quantized vortex in boson systems, Nuovo Cimento 20 (1961) 454.

[18] S. P. Han, A globally convergent method for nonlinear programming, J. Optim. Theory Appl. 22 (1977) 297–309.

[19] C. J. Myatt, E. A. Burt, R. W. Ghrist, E. A. Cornell, C. E. Wieman, Production of two overlapping Bose–Einstein condensates by sympathetic cooling, Phys. Rev. Lett. 78 (1997) 586–589.

[20] L. P. Pitaevskii, Vortex lines in an imperfect Bose gas, Sov. Phys. JETP 13 (1961) 451.

[21] F. Riboli, M. Modugno, Topology of the ground state of two interacting Bose–Einstein condensates, Phys. Rev. A 65 (2002) 063614.

[22] C. Rüegg, N. Cavadini, A. Furrer, H.-U. Güdel, K. Krämer, H. Mutka, A. Wildes, K. Habicht, P. Vorderwisch, Bose–Einstein condensation of the triplet states in the magnetic insulator TlCuCl3, Nature 423 (6935) (2003) 62–65.

[23] B. I. Schneider, D. L. Feder, Numerical approach to the ground and excited states of a Bose–Einstein condensed gas confined in a completely anisotropic trap, Phys. Rev. A 59 (3) (1999) 2232–2242.

[24] E. Timmermans, Phase separation of Bose–Einstein condensates, Phys. Rev. Lett. 81 (1998) 5718–5721.

[25] R. P. Tiwari, A. Shukla, A basis-set based Fortran program to solve the Gross–Pitaevskii equation for dilute Bose gases in harmonic and anharmonic traps, Comput. Phys. Commun. 174 (12) (2006) 966–982.

[26] H. Wang, A time-splitting spectral method for coupled Gross–Pitaevskii equations with applications to rotating Bose–Einstein condensates, J. Comput. Appl. Math. 205 (2007) 88–104.